HHS Public Access

Author manuscript

Nat Immunol. Author manuscript; available in PMC 2014 April 14.

Published in final edited form as:

Nat Immunol. 2012 September ; 13(9): 888–899. doi:10.1038/ni.2370.

Deciphering the transcriptional network of the DC lineage

Jennifer C Miller[1,2], **Brian D. Brown**[1,3], **Tal Shay**[4], **Emmanuel L Gautier**[1,5,6], **Vladimir Jojic**[7,8], **Ariella Cohain**[3], **Gaurav Pandey**[3], **Marylene Leboeuf**[1,2], **Kutlu G Elpek**[9], **Julie Helft**[1,2], **Daigo Hashimoto**[1,2], **Andrew Chow**[1,2,10], **Jeremy Price**[1,2], **Melanie Greter**[1,2,7], **Milena Bogunovic**[1,2], **Angelique Bellemare-Pelletier**[9], **Paul S. Frenette**[10], **Gwendalyn J. Randolph**[1,5,6], **Shannon J. Turley**[9], **Miriam Merad**[1,2], and **the Immunological Genome Consortium**

[1]Immunology Institute, Mount Sinai School of Medicine New York, NY, USA

[2]Department of Oncological sciences, Mount Sinai School of Medicine New York, NY, USA

[3]Institute for Genomics and Multiscale Biology and Department of Genetics and Genomic Sciences, Mount Sinai School of Medicine New York, NY, USA

[4]Broad Institute, Cambridge, MA 02142, USA

[5]Department of Regenerative Biology, Mount Sinai School of Medicine New York, NY, USA

[6]Department of Pathology & Immunology, Washington University in St. Louis, St. Louis, MO, USA

[7]Computer Science department, Stanford University, Stanford, CA

[9]Cancer Immunology and AIDS, Dana Farber Cancer Institute, Boston, MA, USA

[10]Albert Einstein College of Medicine, Bronx, NY

Abstract

Although, much progress has been made in our understanding of DC ontogeny and function, the transcriptional regulation of DC lineage commitment and functional specialization *in vivo* is poorly understood. We performed a comprehensive comparative analysis of CD8+, CD103+, CD11b+, and plasmacytoid DC subsets and the recently identified Macrophage DC precursors and Common DC precursors across the entire immune system. Here we characterize candidate transcriptional activators involved in myeloid progenitor commitment to the DC lineage and predicted regulators of DC functional diversity in tissues. We identify a molecular signature that distinguishes tissue DC from macrophages. We also identify a transcriptional program expressed specifically during steady-state tissue DC migration to the draining lymph nodes that may control tolerance to self-tissue antigens.

Corresponding author: Miriam Merad, M.D., Ph.D., 1425 Madison Avenue, Box 1496, Tel: 212 659 8276, Miriam.merad@mssm.edu.

[8]Present address: Department of Computer Science, UNC, Chapel Hill, NC

Introduction

The Immunological Genome Project (ImmGen) is a consortium of immunologists and computational biologists from multiple institutes who have united to create an exhaustive database of gene expression and regulatory gene networks across the entire murine hematopoietic lineage using the same rigorously controlled data generation pipeline. Utilizing this extensive database, we sought to define the transcriptional profile and regulatory networks that control the dendritic cell (DC) lineage development homeostasis and function.

Discovered only fifty years ago, DC are the most recent addition to the hematopoietic cell lineage[1]. DC represent a small population of hematopoietic cells that share properties with tissue macrophages (MF), including their localization in most tissues, their ability to sample extracellular antigens, sense environmental injuries and contribute to the induction of tissue immune response[1]. However, in contrast to MF whose main role is to scavenge damaged cells or pathogenic microbes and promote tissue repair, the main function of DC is to initiate antigen specific adaptive immune responses against foreign antigens that breach the tissues [2] as well as maintain tolerance to self-antigens [3]. The unique role of DC in adaptive immunity relies on their ability to process and present self and foreign antigens in the form of MHC-class II- and MHC class I-peptide complexes on the cell surface[4,5] together with a superior ability to migrate to the tissue draining lymph nodes (LN) [6] and co-localize with T and B lymphocytes [7]. This makes DC uniquely poised to control the induction of an antigen-specific immune response. Controversies, however, still exist as to the overall distinction between DC and MF due to partially overlapping phenotypse and functions and consequently the exact contribution of MF and DC to tissue immune responses remains debated [8,9]

DC consist of distinct subsets with different abilities to process antigens, respond to environmental stimuli and engage distinct effector lymphocytes [10]. Classical DC (cDC) form the predominant DC subset and are further subdivided into lymphoid tissue resident $CD8^+$ cDC and $CD8^-$ cDC [11]. Lymphoid tissue resident cDC subsets are functionally specialized and $CD8^+$ cDC excel in the cross-presentation of cell associated antigens to $CD8^+$ T cells, whereas $CD8^-$ cDC are the most potent at stimulating $CD4^+$ T cells. The second major subset of DC is called plasmacytoid DC (pDC). pDC are uniquely potent at producing large amounts of the antiviral interferon alpha cytokine and initiate T cell immunity against viral antigens [12]. Non-lymphoid tissue DC also include two cDC subsets, the $CD103^+$ cDC and $CD11b^+$ cDC [13]. Similar to lymphoid tissue $CD8^+$ cDC, non-lymphoid $CD103^+$ cDC are efficient cross-presenters of cell-associated antigens and are the most potent at stimulating $CD8^+$ T cells[10], but may also facilitate the induction of T regulatory cells in the intestine [14].

The successive steps that lead to DC lineage commitment in the bone marrow are starting to be characterized. A myeloid precursors called macrophage and DC precursor (MDP) [15] was recently identified and shown to give rise to monocytes and to the common DC precursor (CDP) [16]. CDP is a clonogenic precursors that has lost monocyte/macrophage differential potential and gives rise exclusively to pDC and cDC [17,18]. CDP also produce pre-cDC, a

circulating cDC restricted progenitor that has lost pDC differentiation potential [16] and home to tissues to differentiate locally into lymphoid tissue resident $CD8^+$ and $CD8^-$ cDC[16] and non lymphoid tissue resident cDC [19]. Although, much progress has been made in our understanding of DC ontogeny and function, the transcriptional regulation of DC lineage commitment, diversification and functional specialization *in vivo* as well as the relationship between lymphoid and non-lymphoid tissue DC remain poorly understood. These questions remain unanswered due, in part, to the limited data available to perform comprehensive, comparative analysis both vertically and horizontally across the immune system.

This study deciphers the transcriptional network of the bone marrow derived DC precursors, the lymphoid tissue and non-lymphoid tissue DC as well as non-lymphoid tissue DC in a migratory state. The results of this study help characterize a DC-specific signature that distinguishes cDC from MF in tissues. Our study also identifies the lineage relationship between different tissue DC subsets as well as the predicted regulators of tissue DC diversity. Our results also uncover a common transcriptional program expressed by all non-lymphoid tissue cDC that migrated to the draining lymph nodes, regardless of their tissue or lineage origin.

Results

Transcriptional characterization of the DC lineage

We characterized 26 distinct DC populations isolated from primary lymphoid tissues, secondary lymphoid tissues and non-lymphoid tissues based on cell surface expression thought to represent discrete DC subsets with specialized immune function *in vivo*[13] (Table 1). Each subset was sorted to high purity according to the ImmGen standard operating protocol. $CD8^+$ and $CD8^-$ cDC and pDC were isolated from the spleen, thymus and LN, $CD103^+$ and $CD11b^+$ cDC were purified from the lung, liver, small intestine and kidney and the epidermal LC were isolated from the epidermis. Tissue migratory $CD103^+$ and $CD11b^+$ DC were isolated from tissue draining LN. Granulocyte macrophage precursors (GMP), macrophage DC precursors (MDP) and common DC precursors (CDP) were purified from the bone marrow, whereas circulating monocytes were isolated from the blood. Cell populations were double sorted based on the cell surface markers described in Table 1 to reach more than 99% purity. The final cytometric sorts (10,000 to 30,000 cells) were performed directly in Trizol, frozen after 2 minutes, and sent to the ImmGen core team in Boston. RNA was prepared from the Trizol lysate and hybridized to the microarray as described in [21]. Expression profiling data were generated on Affymetrix ST1.0 microarrays per ImmGen pipeline, with data generation and quality control as detailed in [21]. The purified DC subsets were isolated from laboratories located in New York (NY) and Boston (MA). One population of spleen DC (population 1, sorted in NYC, NY) was sorted based on MHC II and CD11c expression and lack of F4/80 and B220 expression and found to be identical to spleen DC (population 2, sorted in Boston, MA) purified based mainly on CD11c expression (Supplementary Note 2). To ascertain whether site or batch effects may confound the signals, $CD8^+$ and $CD8^-$ spleen cDC were sorted independently at the two different locations (NY and MA). The data showed excellent correlation within each subset, with

little evidence for lab-specific influences, in relation to the differences between $CD8^-$ and $CD8^+$ cDC subsets (Supplementary Fig. 1).

Transcriptional control of DC lineage commitment

Myeloid lineage commitment to the mononuclear phagocyte lineage is determined at the stage of the MDP, at which point erythroid, megakaryocyte, lymphoid and granulocyte fates have been precluded [15,16,22]. DC commitment occurs during MDP transition to CDP, with the loss of monocyte potential [16], whereas commitment to cDC occurs at the pre-cDC stage with the loss of pDC potential [17,18].

We probed the regulator expression pattern along the myeloid-DC lineage tree to search for transcriptional activators and repressors that correlated with each differentiation step, and thus identified groups of regulators induced at different stages during DC differentiation (see materials and methods). The first group was up-regulated (fold change [FC]≥1.5) specifically during myeloid precursors commitment to the MDP potentially influencing global DC and MF development (Fig. 1a **top**). This group included the transcription factors *Sox4* and *Taf4b* known to play a role, respectively, in cell fate and initiation of transcription. The second group of transcripts was up-regulated (FC≥1.5) during GMP-MDP transition to CDP but not during GMP-MDP transition to circulating monocytes (Fig.1a. **bottom, left and middle panel**) potentially promoting lineage differentiation to DC over monocytes. This group of regulators included the regulators *Irf8, Bcl11a, Runx2, Klf8* and the zinc finger protein *Zbtb46*. A third group of regulator transcripts was down-regulated (FC≤0.67) during GMP-MDP transition and contained the TGF-β induced homeobox gene *Tgif*, the transcription factor *Tcfec* and the E3 ubiquitine ligase *Trim13*. To search for regulators that might contribute to DC lineage diversification, we examined the expression of candidate gene regulators during CDP differentiation to either pDC, lymphoid tissue $CD8^+$ cDC or lymphoid tissue $CD8^-$ cDC (Supplementary Fig. 2, Fig. 1c). CDP differentiation into pDC was associated with the down-regulation of *Id2, Zbtb46* and the TGF-β regulator *Cited2* suggesting that induction of these factors likely contribute to lineage commitment to cDC differentiation. In contrast, CDP differentiation to cDC was associated with the down-regulation of *Irf8, Tcf4, Runx2* and up-regulation of *Batf3, Bcl6* and *Ciita* transcription factors. We further identified regulator transcripts up-regulated (FC≥1.5) in either $CD8^+$ or $CD8^-$ cDC. These transcripts included expected genes such as the $CD8^+CD103^+$-specific transcription factor *Irf8*[19,23] as well as novel genes like hox factor *Pbx1* gene transcript shown to function during definitive hematopoiesis in the fetal liver[24].

Several transcription factors identified in our analysis have been shown to control DC development. For example, pDC and cDC differentiation is dependent on the zinc finger protein Ikaros[25], the cytokine Flt3 ligand and its receptor Flt3 (ref [26]), whose expression is partly controlled by *Pu.1*(*Sfpi1*) [27] and the transcription factor *Stat3*, which is activated upon Flt3 signaling and mediates Flt3 ligand-dependent DC differentiation[28]. Factors that regulate DC diversification are also starting to be identified. The transcription factors *Tcf4* (*E2-2*), *Spib, and Irf8* have been shown to control pDC differentiation [29] whereas *Bcl6* has also been shown to control cDC but not pDC[30] development in the spleen. The transcription factors *Batf3 and Irf8*, the inhibitor of DNA (*Id*) 2 and the mammalian target of rapamycin

(*Mtor*)control the development of $CD8^+$ and $CD103^+$ cDC, while $CD8^-$ cDC differentiation is controlled by the transcription factors *Irf2, Irf4*[8] and *Notch2*[20], a factor that also controls the differentiation of intestinal $CD103^+CD11b^+$ cDC[20]. Consistent with our finding that *Zbtb46* is expressed during transition to CDP and down-regulated during CDP differentiation into pDC, two studies published this week showed that *Zbtb46* transcription factor is restricted to cDC committed precursors and tissue cDC and is absent from pDC, monocytes, macrophages and other myeloid and lymphoid cells[31,32]. *Zbtb46* over-expression in bone marrow progenitor cells inhibited granulocyte potential and promoted cDC development strongly suggesting that *Zbtb46* helps enforce cDC lineage commitment[32] and may serve as a useful marker to distinguish between cDCs and other tissue phagocytes[31,32].

Altogether, these results provide a map of known regulators but also unknown potential regulators that accompany key cellular checkpoints of DCpoiesis and help identify the molecular cues that control monocyte/DC lineage differentiation as well as DC diversification *in vivo*.

Identification of a cDC core gene signature

One of the major challenges to understanding the exact contribution of cDC versus MF in tissue immunity has been the lack of specific phenotypic markers to define tissue cDC. We first ascertained whether cDC and MF sorted based on published markers clustered as one or separate populations by performing a principal component analysis (PCA) of the top 15% most variable genes expressed by different steady-state leukocytes isolated from the same organ in the steady-state (Supplementary Fig. 1d). These results revealed that MF and cDC form distinct populations at the transcriptome level.

We then asked whether cDC expressed a set of transcripts that are present in all cDC subsets, but absent from MF. As non-lymphoid tissue $CD11b^+$ cDC likely form a heterogeneous population[8,9], we excluded non-lymphoid tissue $CD11b^+$ cDC from the comparative analysis and asked whether lymphoid tissue $CD8^+$ cDC and $CD8^-$ cDC and non-lymphoid tissue $CD103^+$ cDC shared specific cDC transcripts that were absent from four prototypical MF populations profiled by the ImmGen group as described in methods. Twenty-four transcripts were differentially expressed ($FC \geq 2$; t-test false discovery rate [FDR]≤ 0.05) in cDC and absent from MF as determined by expression values below QC95, or the value at which the transcript has a 95% chance of being expressed (Fig. 2a, Table 2). This group of transcripts form the “core cDC signature” and includes the chemokine receptor *Ccr7* shown to control cDC migration to the draining lymph nodes[33], the zinc finger protein *Zbtb46*, which is first up-regulated at the CDP stage (Fig. 1a), and, *Flt3* that encodes the receptor for the cytokine Flt3 ligand receptor known to control DC differentiation and homeostasis[22,34]. Although many of the genes transcripts enriched in cDC and absent in MF were also found in other hematopoietic cell populations, *Zbtb46*, *Flt3*, as well as *Pvrl1* and *Anpep (Cd13)* were significantly up-regulated in cDC compared to all other hematopoietic cell subsets (Fig. S3; Table S1). Strikingly, many transcripts had no identified role in cDC biology, such as *Kit*, the receptor for kit ligand (stem cell factor) known for its role in hematopoiesis as well as mast cell differentiation[35], and *Btla* (CD272),

an Immunoglobulin superfamily member that attenuates B cell and T cell receptor-mediated signaling [36]. *Btla* was specifically up-regulated in $CD8^+$ $CD103^+$ cDC populations in comparison to $CD8^-$ cDCs (Fig. 2a-b, Fig. S3, Table S1). Several transcripts were up-regulated (FC≥2; t-test FDR≤0.05) in cDC compared to MF including multiple class II genes and *Dpp4* (*CD26*) (Fig. 2a, Table 3), whose role in DC function remains unclear. Using flow cytometry, we confirmed that Flt3, c-Kit, BTLA and CD26 were expressed at the protein level on spleen $CD8^+$, spleen $CD8^-$ cDC as well as non-lymphoid tissue $CD103^+$ cDC and absent from red pulp MF, lung alveolar MF, peritoneal MF and microglia (Fig. 2b). Altogether these results identify a core DC signature that helps distinguish tissue DC from MF in tissues.

Unique gene signatures characterize distinct tissue DC clusters

DC subsets are classified based on distinct cell surface markers and different subsets exist in lymphoid and non-lymphoid tissues. To understand the relationship between these different DC populations, we performed a PCA of the top 15% most variable genes of lymphoid tissue pDC (spleen, skin draining LN and mesenteric LN pDC), lymphoid tissue cDC (LN, spleen, thymic $CD8^+$ cDC; LN, spleen $CD8^-CD4^+$ cDC; spleen $CD8^-CD4^-CD11b^+$cDC) and non-lymphoid tissue $CD103^+$ cDC (lung, liver, and small intestine) populations. The main principal components identified three distinct DC clusters (Fig. 3a). One cluster was formed by lymphoid tissue $CD8^+$ and non-lymphoid tissue $CD103^+$ cDC (Fig. 3a). A second cluster was formed by lymphoid tissue $CD8^-$ cDC, whereas a third cluster was formed by pDC (Fig. 3a). We used these clusters to define specific gene expression signatures. The pDC cluster expressed 93 gene transcripts absent from other cDC, whereas the two cDC clusters expressed 125 gene transcripts absent from pDC including *Zbtb46*, *Pvrl1*, and *Anpep (Cd13*) (Fig. 3b; Supplementary Fig. 4; Supplementary Table 1). Further analysis of the two cDC subsets revealed 28 gene transcripts shared by $CD8^+$ and $CD103^+$ cDC and absent from other cDC (Fig. 3b; Supplementary Fig. 3-4; Supplementary Table 1). $CD8^+$ and $CD103^+$ cDC specific gene transcripts included *Tlr3*, the chemokine receptor *Xcr1*. In agreement with their unique TLR3 expression, $CD8^+$ DC and $CD103^+CD11b^-$ DC share a superior ability to respond to TLR3 ligand adjuvant [37-40]. In addition, recent data revealed that $CD8^+$ DC are also the only lymphoid tissue DC subset that produces interferon lambda in response to the TLR3 ligand Poly I:C [41] and similar results were found for lung $CD103^+CD11b^-$ DC (Helft and Merad unpublished). Remarkably, *Xcr1*, which controls $CD8^+$ T effector cell differentiation in mice and human [42,43], is expressed only in $CD8^+CD103^+$ cDC across the entire hematopoietic cell lineage (Supplementary Fig. 4c, Supplementary Table 1). Lymphoid tissue $CD8^-$ cDC populations co-expressed core cDC gene transcripts together with several monocyte and MF gene transcripts (Supplementary Fig. S4, Supplementary Table 1), which is consistent with recent results from our laboratory showing that $CD8^-$ cDC consist of two subsets that differentially expressed MF related genes[20]. However, some genes including *Dscam* (down syndrome cell adhesion molecule) were uniquely expressed by $CD8^-$ cDC and absent from macrophages and monocytes (Supplementary Fig. 4, Supplementary Table 1). Dscam is a molecule with enormous molecular diversity which plays a role in axon guidance [44] and also functions as an immuno-receptor able to recognize diverse pathogens in drosophila [45]

To dissect the gene architecture program of these subsets of DC, we searched among the 334 fine modules of strongly co-expressed genes and predicted regulators identified for the entire ImmGen compendium (http://www.immgen.org/ModsRegs/modules.html) to identify those that were significantly up-regulated in specific DC subsets in comparison to the rest of the ImmGen samples (material and methods) (Fig. 3c-e). Module 150 was significantly up-regulated in pDC (p=4.77*10^{-11}) and predicted regulators of this module included *Irf8, Stat2, Runx2*, and *Tsc22d1* (Fig. 3c), which were also expressed during CDP commitment to pDC (Fig. 1b). Module F156 was significantly up-regulated in cDC (p=7.01*10^{-35}) and enriched in core cDC genes (p=4.18*10^{-10}; hypergeometric test) such as *Zbtb46* and *Pvrl1*. Predicted regulators of this module included *Batf3* and *Relb* (Fig. 3d), which were also up-regulated during DC commitment to cDC (Fig. 1b). Module 152 was significantly up-regulated in CD8$^+$ CD103$^+$ cDC (p=1.34*10^{-25}) and enriched in CD8$^+$ CD103$^+$ DC transcript signature (p<*10^{-13}, hypergeometric test) such as *Tlr3, Xcr1* and *Fzd1* (Fig. 3e). *Irf8* and *Pbx1* also identified during CDP commitment to CD8$^+$ cDC (Fig. 1b) were predicted regulators of this module (Fig. 3e). Module 154 was significantly up-regulated in CD8$^-$ cDC (p=1.08*10^{-15}) and in intestinal CD103$^+$ CD11b$^+$ cDC, a non-lymphoid tissue cDC subset recently shown to share development properties with lymphoid tissue CD8$^-$ cDC[20] (Supplementary Fig. 5). These modules together with the core gene signature identify novel genes as well as potential regulators of DC functional specialization *in vivo*.

The cDC core gene signature helps decipher tissue CD11b$^+$ DC heterogeneity

Non-lymphoid tissue CD11b$^+$ cDC remain the least well characterized cDC subset both ontogenically and functionally. The small intestine is populated by three phenotypically distinct cDC subsets that differentially express the integrins CD103 and CD11b. CD103$^+$CD11b$^-$ cDC and CD103$^+$CD11b$^+$ cDC are derived from the CDP and pre-DC [46,47], require FLT3 ligand for their development [47], migrate efficiently to the draining LN [48] and are thought to represent cDC [49]. In contrast, the CD103$^-$ CD11b$^+$ subset derives from circulating monocytes [46,47], develops independently of FLT3 ligand, requires CSF-1R ligand for its development [47] migrates poorly to the draining LN [48] and is thought to relate more closely to MF than to cDC [49].

To examine whether the core cDC signature identified above is differentially expressed by these subsets, we purified CD103$^+$CD11b$^-$, CD103$^+$CD11b$^+$ and CD103$^-$CD11b$^+$ small intestine (SI) cDC subsets as well as lung, liver and kidney CD11b$^+$ cDC, and reran a PCA with the rest of the cDC subsets and with MF isolated from the spleen, lung, brain and peritoneum. CD11b$^+$ cDC subsets were distributed across the PCA between the cDC and MF (Fig. 4a) and expressed a variable number of cDC core genes (Fig. 4b) indicating that non-lymphoid tissue CD11b$^+$ cDC as currently defined, represent a heterogenous population.

CD103$^+$CD11b$^-$ SI cDC clustered with the CD8$^+$ CD103$^+$ cDC, whereas lamina propria CD103$^+$CD11b$^+$ SI cDC clustered near lymphoid CD8$^-$ cDC and did not express CD8$^+$ CD103$^+$ cDC unique transcripts (Fig. 4a, Supplementary Fig. 6). Accordingly, CD103$^+$CD11b$^-$ SI cDC expressed all CD8$^+$CD103$^+$ cDC specific transcripts identified (Fig. 3), including *Fzd1* a Wnt receptor signaling which controls β-catenin activation and

translocation to the nucleus (Supplementary Fig. 4, 6). *Fzd1* was expressed specifically in $CD103^+CD11b^-$ SI cDC and was absent from $CD103^+CD11b^+$ cDC and $CD103^-CD11b^+$ SI cDC (Supplementary Fig. 6). β-catenin activation and translocation to the nucleus can control the ability of DCs to promote T cell tolerance in the intestine[50]. It will be important to examine the contribution of *Fzd1* and $CD103^-CD11b^+$ SI cDC to T cell immune modulation in the gut.

In contrast, the $CD103^-CD11b^+$ cDC clustered close to MF and away from other DC (Fig. 4a). Consistent with the PCA results, we found that $CD103^+CD11b^-$ and $CD103^+CD11b^+$ SI DC expressed 100% of the core cDC genes as well as the cDC specific proteins c-Kit, Flt3, BTLA and CD26 on the cell surface (Fig. 4b-d, Fig. S6) suggesting that these two subsets belong to the DC lineage. In contrast, $CD103^-CD11b^+$ cDC clustered close to MF and away from cDC, they expressed only 40% of the core cDC genes and lacked the cDC proteins Kit, Flt3, BTLA and CD26 on the cell surface (Fig. 4b-d; Supplementary Fig. 6) suggesting that small intestine $CD103^-CD11b^+$ cDC belong to the MF lineage. Accordingly, a focused analysis of MF-associated transcripts indicated that the $CD103^-CD11b^+$ cDC SI population clustered with MF (Gautier et al., in preparation). Altogether, these results establish that the current DC phenotypic definition, which is based on MHC class II and CD11c expression, is not sufficient to identify tissue DC; and the use of the cDC gene signature provides a new means to distinguish $CD11b^+$ cDC from MF in non-lymphoid tissues.

Migratory DC display a unique transcriptional signature

Tissue draining LN contain blood-derived DC that include pDC, $CD8^+$ cDC and $CD8^-$ cDC also called LN resident DC as well as non-lymphoid tissue $CD103^+$ cDC and $CD11b^+$ cDC that have migrated from the drained tissue also called “tissue migratory cDC” [6]. The mechanisms that control non-lymphoid tissue cDC migration and function in the draining LN in response to tissue injury or tissue immunization are starting to be unraveled; however, far less is known about the gene program that controls cDCs ability to leave peripheral tissues and migrate to the draining LN or the gene regulators that control migratory cDC immune function in the non-inflamed state [6]. Here we analyzed the transcriptional program of tissue cDC prior to their migration to the draining LN (parent DC population) and upon migration to the LN as well as LN resident cDCs. Strikingly, we found that migratory cDC segregated together irrespective of their cellular or tissue origin and away from parent cDC populations that populate the drained tissue (Fig. 5a) and expressed a very similar transcriptional program (Fig. 5b-e). $CD11b^+$ migratory cDC clustered together with $CD103^+$ migratory cDC suggesting that among tissue $CD11b^+$ cDC those that migrated in the steady state may represent the “bonafide” cDC. In addition, we found that in contrast to tissue $CD11b^+$ cDC, which expressed moderate amounts of the DC specific gene *Flt3*, migratory $CD11b^+$ cDC always expressed high *Flt3* levels. Specifically, epidermal Langerhans cells (LC), which develop independently of Flt3 and Flt3L [19] and express very low amounts of *Flt3* in tissue, dramatically up-regulated *Flt3* transcripts once they reach the LN (Supplementary Fig. 7), suggesting that Flt3 plays a critical role in the homeostasis or function of steady state migratory cDC.

We also found that tissue migratory cDC up-regulated some gene transcripts dedicated to the dampening of immune responses (Fig. 6). As dampening genes can also be up-regulated in response to injury, we further compared steady state migratory cDC with Poly I:C activated cDC (Fig. 6a). As expected, Poly I:C activated and steady state tissue migratory cDC up-regulated the co-stimulatory gene transcript *Cd40*, previously reported on steady state migratory LC[51] (Fig. 6a); however, steady state migratory cDC failed to up-regulate inflammatory cytokine transcripts (Fig. 6b) and expressed higher levels of immunomodulatory transcripts compared to Poly:I:C activated cDC (Fig. 6a). Immunomodulatory transcripts up-regulated in steady state migratory cDC included genes known to suppress T cell function either directly such as *Cd274* (*Pd-l1*) [52], or via the production or activation of immunosuppressive cytokines such as the TGF-β activating integrin Itgb8[53]. Other up-regulated transcripts encoded proteins known to reduce DC activation and cytokine production including *Socs2*, a TLR–responsive gene which regulates DC cytokine release via STAT3 modulation[54], *Pias3*, also known to modulate STAT3 phosphorylation and NF-κB expression[55], and *Cd200*, a protein known to reduce pro-inflammatory DC activation upon binding to its receptor, which is also expressed on DC[56]. Furthermore, steady state migratory cDC up-regulated transcripts important in reducing DC survival including cell death receptor *Fas* [57,58]. Using flow cytometry and immunofluorescence analysis, we confirmed protein expression of *Fas*, *Cd200*, *Pd-l1*, and *Pias3* and the co-stimulatory molecule *Cd40* in steady state tissue migratory cDC (Fig. 6c-d). Based on these data we will speculate that cDC that leave the non-lymphoid tissues in the steady state upregulate a transcriptional immunomodulatory program that may prevent the induction of adaptive immune response to self- tissue antigens. The functional relevance of the immunomodulatory migratory DC signature needs to be confirmed experimentally.

Discussion

This study provides the first comprehensive comparative analysis of DC precursors and tissue DC transcriptome across the entire immune system. The results of this study help identify: a transcriptional network that accompanies DC lineage commitment and diversification; a DC-specific signature that distinguishes cDC from MF in tissues; the relationship between lymphoid and non-lymphoid tissue DC subsets and predicted regulators of DC diversity; and a transcriptional immunomodulatory program expressed specifically during steady state tissue DC migration to the draining LN.

To gain knowledge of the transcriptional network that controls myeloid commitment to the DC lineage, we analyzed the transcriptional network associated with three key DC differentiation checkpoints: CMP ➔MDP, MDP ➔ CDP and CDP ➔ pDC $CD8^+$ cDC or $CD8^-$ cDC. This analysis identified a group of transcriptional activators that include *Zbtb46*, *Runx2*, *Bcl11a* and *Klf8* that rose specifically during MDP commitment to CDP but not monocytes suggesting their potential key role in driving myeloid commitment to the DC restricted precursors and away from monocytes *in vivo*. We also characterized the transcriptional networks that accompany CDP differentiation into pDC, $CD8^+$ cDC and $CD8^-$ cDC subsets and identify several gene candidates that may drive DC lineage diversification *in vivo*.

One of the main controversies in the DC literature is the distinct contribution of cDC versus MF to tissue immunity. This confusion is partly a consequence of the paucity of markers available to distinguish between these two cell types leading researchers to use promiscuous markers such as MHC class II, CD11c and F4/80 to assess cDC or MF specific function[9]. We identified a core cDC gene signature shared by lymphoid tissue $CD8^-$ and $CD8^+$ cDC, and non-lymphoid tissue $CD103^+$ cDC and absent from tissue MF. cDC-specific transcripts included the gene coding for Zbtb46, Flt3, Kit and CCR7. The identification of the *Kit* transcript as part of the cDC gene specific signature is surprising, as *Kit* and its ligand have never been shown to play an intrinsic role in cDC development *in vivo*. Future studies will be needed to identify the role, if any, of Kit in DC differentiation, function and homeostasis *in vivo*. Importantly, the use of the cDC gene signature helped delineate the heterogeneity of non-lymphoid tissue $CD11b^+$ cDC and identify a contaminating MF population, which could not have been detected using phenotypical markers currently used to define DC populations *in vivo*.

We also established that among cDC, lymphoid tissue $CD8^+$ cDC and non-lymphoid tissue $CD103^+$ cDC shared a gene signature, regardless of the tissue environment in which they reside. $CD8^+$ $CD103^+$ cDC gene signature was absent from the rest of DC including pDC, $CD8^-$ cDC and $CD103^-$ cDC in these same tissues. These results establish $CD8^+$ $CD103^+$ cDC as a distinct lineage subset and identify the gene regulators that may drive their differentiation, homeostasis and function. Using the novel algorithm termed Ontogenet developed for the ImmGen dataset (Jojic et al, in preparation), we identified modules of strongly co-expressed genes that were specifically and differentially expressed in each DC subset. Specifically we show that modules F150, F156 and F152 are up-regulated in pDC, cDC and $CD8^+$ $CD103^+$ cDC respectively and identify candidate regulatory programs that predict their expression pattern and therefore may drive DC functional specialization *in vivo*.

Strikingly, we found that regardless of tissue or cellular origin, non-lymphoid tissue $CD103^+$ cDC and $CD11b^+$ cDC as well as epidermal LC that migrate to the draining LN in the steady state up-regulate a shared gene signature. Some of the highest up-regulated transcripts are implicated in DC production of immunosupressive cytokine, the dampening of DC activation and reduction of DC survival that is known to lead to the dampening of T cell activation. These results are consistent with the potential role of steady state migratory cDC in the induction or maintenance of T regulatory response[3] and identify candidate molecules that may participate in the control tolerance to self-antigens *in vivo*.

The results of this study provide a comprehensive characterization of the DC lineage transcriptional network and should help the development of novel genetic tools such as inducible gene regulation *in vivo* and lineage tracing of genetically marked defined myeloid precursor populations to further comprehend the developmental complexity of the phagocyte system. Moreover, the availability of the ImmGen datasets will now permit further investigations into DC gene expression networks and help unravel the transcriptional program that control DC function in the steady and injured state.

Methods

Mice

All cells analyzed in this study were obtained from six-week-old male C57BL/6J mice purchased from Jackson Laboratory with exception of LC and Mig LC which were isolated from Langerin EGFP C57BL/6J mice [59]. All mice were housed in specific pathogen–free facilities at the Mount Sinai School of Medicine facility. Experimental procedures performed in mice were approved by the Animal Care and Use Committee of the Mount Sinai School of Medicine.

Cell sorting and flow cytometry

All cells were purified using the ImmGen Standardized Sorting protocol and antibodies listed on http://www.ImmGen.org. Sorting was performed at the Mount Sinai Flow Cytometry Shared Resource Facility using the Aria II (BD) or Influx (BD). Marker combination used to sort specific populations are available on http://www.ImmGen.org. Multiparameter analysis of stained cell suspensions were performed on LSRII (BD) and analyzed with FlowJo software (Tree Star, Inc). Monoclonal antibodies (mAbs) specific to mouse CD8 (clone 53-6.7), CD4 (clone L3T4), CD45 (clone 30-F11), CD11c (clone N418), CD11b (clone M1/70), I-A/I-E (clone M5/114.15.2), CD103 (clone 2E7), CD117/c-Kit (clone 2B8), CD135/Flt3 (clone A2F10), CD26 (clone H1940112), BTLA/CD272 (clone 6F7), CD40 (clone HM40-3), CD95/Fas (clone Jo2), CD200 (clone OX90), PD-L1/CD274 (clone MIH5), and the corresponding isotype controls were purchased from eBioscience or BD.

Cytospin and immunofluorescence of sorted cells

Viable sorted cells isolated according to MHCII and CD11c expression were sorted, Cytospun onto glass slides, and dried overnight. Slides were fixed for 1 hr with 4% paraformaldehyde in PBS, blocked with 10% goat serum in 0.1% Triton/0.1% BSA in PBS for 1 hr, then stained for 48 hrs at 4°C followed by 1 hr incubation at room temperature (RT) with the goat anti- mouse Pias3 mAb (Sigma, clone P0117) at 1:2000 dilution. Secondary goat anti-mouse Alexa Fluor594 (Invitrogen) was added to slides for 1 hr at RT. Slides were mounted with DAPI in Fluoro-gel with Tris buffer (Electron Microscopy Sciences). Images were acquired at 63× using the Zeiss Axioplan2IE with a Zeiss AxioCam MRc and analyzed using the Zeiss AxioVision software.

Microarray analysis, normalization and dataset analysis

RNA was prepared from sorted cell populations from C57BL/6J mice using Trizol reagent as described[60]. RNA was amplified and hybridized on the Affymetrix Mouse Gene 1.0 ST array according to the manufacturer's procedures. Raw data for all populations were preprocessed and normalized using the RMA algorithm [61] implemented in the “Expression File Creator” module in the GenePattern suite [62]. All datasets have been deposited at the National Center for Biotechnology Information/Gene Expression Omnibus under accession number GSE15907 (http://www.ncbi.nlm.nih.gov/geo/query/acc.cgi?acc=GSE15907). RNA processing and microarray analysis with the Affymetrix MoGene 1.0 ST array was prepared

according to ImmGen standard operating procedures (http://www.immgen.org/Protocols/ImmGen).

Identification of transcription factors associated with DC lineage commitment and diversification

Dataset was filtered for regulators [63] with a coefficient of variation (CV) <0.5 within population replicates. MDP regulators were selected for transcripts expressed 1.5 fold greater than GMP and CDP. CDP regulators were filtered for transcripts expressed 1.5 greater or 0.67 fold less than the precursors MDP and/or GMP. The “MDP and/or GMP” classification allows inclusion of transcripts that may be increasing in the MDP population as well and thus still informative. These were further filtered for expression at least 1.5 fold greater or 0.67 fold less than the nearest neighbor monocytes to find up-regulated or down regulated transcripts important in the DC lineage alone. Gene lists were input into the GenePattern module ExpressCluster (http://cbdm.hms.harvard.edu/resources.html) to identify patterns of expression across the GMP, MDP, CDP and monocyte populations.

Dataset was filtered for regulators with a CV <0.5 within these populations [63]. Differentiated DC subsets were compared to their nearest developmental neighbor using a two-way analysis of variance Student's t-test on normalized expression data corrected with the Benjamini and Hochberg false discovery rate <0.05 and further selected for transcripts up-regulated by at least 1.5 fold within each organ. Thus, pDC were compared to $CD8^+$/$CD8^-$ cDC and $CD8^+$ cDC were compared to $CD8^-$ cDC within spleen, MLN, and SDLN DC and filtered for transcripts up-regulated at least 1.5 fold in each comparison. pDC and cDC were then compared to their precursor CDP to identify transcripts decreased at least 1.5 fold from the precursor. Transcripts up-regulated or expressed at the same level as CDP (red arrow) whereas transcripts downregulated compared to the CDP (blue arrows) are shown.

Generation of the cell specific gene signatures

Differentially expressed transcripts were calculated using an unpaired two-way analysis of variance Student's t-test on normalized expression data. The t-test was controlled for multiple hypothesis using Benjamini and Hochberg false discover rate <0.05. The dataset was then filtered for those probes for which the fold change of any single population mean of the inclusion group over any single population mean of the exclusion group was ≥2 to create signatures of up-regulated transcripts. The dataset was further filtered for transcripts in which, the exclusion populations had an expression value less than the QC value of 95, or the level at which each population would have a predicted 95% certainty of expressing the gene. These gene signatures were also analyzed for variance across all steady-state leukocyte populations using the ANOVA command “aov “in R. Data were log transformed before analysis. Post-hoc pairwise Student's t- tests were run on each population corrected for multiple hypotheses testing using the Bonferroni adjustment. Data are provided in Table S1.

Generation of the migratory DC gene signature

Dataset was filtered for transcripts with a CV <0.5 within population replicates. For creation of the migratory DC signature, the migratory LC, lung CD103+ cDC, and lung CD11b+

cDC samples were directly compared to their tissue resident equivalents and selected for transcripts with a FC≥2 which satisfied the Student's t-test p <0.05. To remove any potential signature that could be created by the lymph node environment, the remaining transcripts were compared in the migratory vs resident SDLN populations again selecting for transcripts at least 2 fold increased which satisfied the t-test p <0.05. This same method was applied to transcripts with a FC ≤ 0.5 which satisfied the t-test p <0.05 to identify a down-regulated signature. This analysis was performed in the GenePattern module Multiplot [64].

Generation of gene modules and prediction of module regulators

The expression data normalization was done as part of the ImmGen pipeline, March 2011 release. Data were log2 transformed. For gene symbols represented on the array with more than one probeset, only the probeset with the highest mean expression was retained. Of those, only the 7996 probesets displaying a standard deviation higher than 0.5 across the entire dataset were used for the clustering.

Clustering was performed by Super Paramagnetic Clustering [65] with default parameters, resulting in 80 stable clusters. The remaining unclustered genes were grouped into a separate cluster (C81). Those are referred to in the text as coarse modules C1-C81. Each coarse cluster was further clustered by hierarchical clustering into more fine clusters, resulting in 334 fine modules, referred to in the text as fine modules F1-F334. The expression of each gene was standardized by subtraction of the mean and division by its standard deviation across all dataset. Replicates were averaged. Mean expression of each module was projected on the tree. Expression values are color coded from minimal (blue) to maximal (red).

A novel algorithm termed Ontogenet was developed for the ImmGen dataset (Jojic et al, in preparation). Ontogenet finds a regulatory program for each coarse and fine module, based on regulators expression and the structure of the lineage tree. One sided two-sample Kolmogorov-Smirnov test was applied to the mean expression of each of the ImmGen fine modules to identify modules with significantly induced expression in specific cell groups. The cell groups were pDC, cDC, CD8- DC and CD8+/CD103+. Background for each was the rest of the ImmGen samples. Benjamini Hochberg FDR <= 0.05 was applied to the p-value table of all four groups across all fine modules. Hypergeometric test for two groups was used to estimate the enrichment of ImmGen fine modules for the four gene signatures. Benjamini Hochberg FDR <= 0.05 was applied to the p-value table of all four groups across all fine modules.

Data analysis and visualization tools

Signature transcripts were clustered and visualized with “HeatMap Viewer” or the “Hierarchical Clustering” tool using Gene Pattern [64]. For hierarchical clustering, data were log scaled, centered around the mean, and clustered using Pearson correlation as a measure and pairwise complete-linkage clustering as a linkage type. Data were centered on rows before visualization. Principal component analysis (PCA) was performed using the Immgen PopulationDistances PCA program (http://cbdm.hms.harvard.edu/resources.html). Where indicated, the PCA program was used to identify the 15% most differentially expressed genes among subsets by filtering based on a variation of analysis using the geometric

standard deviation of populations to weight genes that vary in multiple populations. Data were log transformed, gene and subset normalized, and filtered for transcripts with a CV<0.5 in each set of sample replicates before visualization. Fold change vs fold change and fold change vs t test p-value were visualized using the “Multiplot” module from Gene Pattern [64]. Graphs of individual genes were created utilizing Prism Software.

Supplementary Material

Refer to Web version on PubMed Central for supplementary material.

Acknowledgments

We thank all of our colleagues in the ImmGen and especially the technical team including Micho Painter, Jeff Ericson and Scott Davis for their critical contribution. We are extremely grateful to Christophe Benoist for his critical contribution to the design and writing of the manuscript. The full list of the ImmGen Consortium participants can be found on the ImmGen website. We also thank eBioscience and Affymetrix for material support of the ImmGen Project. ImmGen is funded by R24 AI072073 from NIH/NIAID, spearheaded by Christophe Benoist. Additional support for the present body of work was funded by AI080884 and HL086899 to MM; JDRF172010770 and DP2DK083052-01 to B.D.B; DK074500 and AI045757 to S.J.T. HL69438, DK056638, HL097819 and HL097700 to P.S.F and U54CA149145 to V.J.

References

1. Banchereau J, Steinman RM. Dendritic cells and the control of immunity. Nature. 1998; 392:245–252. [PubMed: 9521319]
2. Steinman RM, Banchereau J. Taking dendritic cells into medicine. Nature. 2007; 449:419–426. [PubMed: 17898760]
3. Steinman RM, Hawiger D, Nussenzweig MC. Tolerogenic dendritic cells. Annu Rev Immunol. 2003; 21:685–711. [PubMed: 12615891]
4. Guermonprez P, Valladeau J, Zitvogel L, Thery C, Amigorena S. Antigen presentation and T cell stimulation by dendritic cells. Annu Rev Immunol. 2002; 20:621–667. [PubMed: 11861614]
5. Trombetta ES, Mellman I. Cell biology of antigen processing in vitro and in vivo. Annu Rev Immunol. 2005; 23:975–1028. [PubMed: 15771591]
6. Randolph GJ, Angeli V, Swartz MA. Dendritic-cell trafficking to lymph nodes through lymphatic vessels. Nat Rev Immunol. 2005; 5:617–628. [PubMed: 16056255]
7. Cyster JG. Chemokines and the homing of dendritic cells to the T cell areas of lymphoid organs. J Exp Med. 1999; 189:447–450. [PubMed: 9927506]
8. Hashimoto D, Miller J, Merad M. Dendritic cell and macrophage heterogeneity in vivo. Immunity. 2011; 35:323–335. [PubMed: 21943488]
9. Geissmann F, Gordon S, Hume DA, Mowat AM, Randolph GJ. Unravelling mononuclear phagocyte heterogeneity. Nat Rev Immunol. 2010; 10:453–460. [PubMed: 20467425]
10. Heath WR, Carbone FR. Dendritic cell subsets in primary and secondary T cell responses at body surfaces. Nat Immunol. 2009; 10:1237–1244. [PubMed: 19915624]
11. Shortman K, Heath WR. The CD8+ dendritic cell subset. Immunol Rev. 2010; 234:18–31. [PubMed: 20193009]
12. Reizis B, Bunin A, Ghosh HS, Lewis KL, Sisirak V. Plasmacytoid dendritic cells: recent progress and open questions. Annu Rev Immunol. 2011; 29:163–183. [PubMed: 21219184]
13. Helft J, Ginhoux F, Bogunovic M, Merad M. Origin and functional heterogeneity of non-lymphoid tissue dendritic cells in mice. Immunol Rev. 2010; 234:55–75. [PubMed: 20193012]
14. Coombes JL, Powrie F. Dendritic cells in intestinal immune regulation. Nat Rev Immunol. 2008; 8:435–446. [PubMed: 18500229]
15. Fogg DK, et al. A clonogenic bone marrow progenitor specific for macrophages and dendritic cells. Science. 2006; 311:83–87. [PubMed: 16322423]

16. Liu K, et al. In Vivo Analysis of Dendritic Cell Development and Homeostasis. Science. 2009
17. Onai N, et al. Identification of clonogenic common Flt3+M-CSFR+ plasmacytoid and conventional dendritic cell progenitors in mouse bone marrow. Nat Immunol. 2007; 8:1207–1216. [PubMed: 17922016]
18. Naik SH, et al. Development of plasmacytoid and conventional dendritic cell subtypes from single precursor cells derived in vitro and in vivo. Nat Immunol. 2007; 8:1217–1226. [PubMed: 17922015]
19. Ginhoux F, et al. The origin and development of nonlymphoid tissue CD103+ DCs. J Exp Med. 2009; 206:3115–3130. [PubMed: 20008528]
20. Lewis KL, et al. Notch2 Receptor Signaling Controls Functional Differentiation of Dendritic Cells in the Spleen and Intestine. Immunity. 2011
21. Malhotra D, et al. Transcriptional profiling of stroma from inflamed and resting lymph nodes defines immunological hallmarks. Nat Immunol. 2012; 13:499–510. [PubMed: 22466668]
22. Waskow C, et al. The receptor tyrosine kinase Flt3 is required for dendritic cell development in peripheral lymphoid tissues. Nat Immunol. 2008; 9:676–683. [PubMed: 18469816]
23. Aliberti J, et al. Essential role for ICSBP in the in vivo development of murine CD8alpha + dendritic cells. Blood. 2003; 101:305–310. [PubMed: 12393690]
24. DiMartino JF, et al. The Hox cofactor and proto-oncogene Pbx1 is required for maintenance of definitive hematopoiesis in the fetal liver. Blood. 2001; 98:618–626. [PubMed: 11468159]
25. Wu L, Nichogiannopoulou A, Shortman K, Georgopoulos K. Cell-autonomous defects in dendritic cell populations of Ikaros mutant mice point to a developmental relationship with the lymphoid lineage. Immunity. 1997; 7:483–492. [PubMed: 9354469]
26. McKenna HJ, et al. Mice lacking flt3 ligand have deficient hematopoiesis affecting hematopoietic progenitor cells, dendritic cells, and natural killer cells. Blood. 2000; 95:3489–3497. [PubMed: 10828034]
27. Carotta S, et al. The Transcription Factor PU.1 Controls Dendritic Cell Development and Flt3 Cytokine Receptor Expression in a Dose-Dependent Manner. Immunity. 2010; 32:628–641. [PubMed: 20510871]
28. Laouar Y, Welte T, Fu XY, Flavell RA. STAT3 is required for Flt3L-dependent dendritic cell differentiation. Immunity. 2003; 19:903–912. [PubMed: 14670306]
29. Reizis B. Regulation of plasmacytoid dendritic cell development. Curr Opin Immunol. 2010; 22:206–211. [PubMed: 20144853]
30. Ohtsuka H, et al. Bcl6 is required for the development of mouse CD4+ and CD8alpha+ dendritic cells. Journal of Immunology. 2011; 186:255–263.
31. Meredith MM. Expression of the zinc finger transcription factor zDC (Zbtb46, Btbd4) defines the classical dendritic cell lineage. J Exp Med. 2012
32. Satpathy AT, et al. Zbtb46 expression distinguishes classical dendritic cells and their committed progenitors from other immune lineages. J Exp Med. 2012
33. Ohl L, et al. CCR7 governs skin dendritic cell migration under inflammatory and steady-state conditions. Immunity. 2004; 21:279–288. [PubMed: 15308107]
34. Lyman SD, et al. Identification of soluble and membrane-bound isoforms of the murine flt3 ligand generated by alternative splicing of mRNAs. Oncogene. 1995; 10:149–157. [PubMed: 7824267]
35. Broxmeyer HE, et al. The kit receptor and its ligand, steel factor, as regulators of hemopoiesis. Cancer Cells. 1991; 3:480–487. [PubMed: 1726456]
36. del Rio ML, Lucas CL, Buhler L, Rayat G, Rodriguez-Barbosa JI. HVEM/LIGHT/BTLA/CD160 cosignaling pathways as targets for immune regulation. J Leukoc Biol. 2010; 87:223–235. [PubMed: 20007250]
37. Hochrein H, et al. Differential production of IL-12, IFN-alpha, and IFN-gamma by mouse dendritic cell subsets. J Immunol. 2001; 166:5448–5455. [PubMed: 11313382]
38. Sung SS, et al. A major lung CD103 (alphaE)-beta7 integrin-positive epithelial dendritic cell population expressing Langerin and tight junction proteins. J Immunol. 2006; 176:2161–2172. [PubMed: 16455972]

39. Longhi MP, et al. Dendritic cells require a systemic type I interferon response to mature and induce CD4+ Th1 immunity with poly IC as adjuvant. J Exp Med. 2009; 206:1589–1602. [PubMed: 19564349]
40. Jelinek I, et al. TLR3-specific double-stranded RNA oligonucleotide adjuvants induce dendritic cell cross-presentation, CTL responses, and antiviral protection. J Immunol. 2011; 186:2422–2429. [PubMed: 21242525]
41. Lauterbach H, et al. Mouse CD8alpha+ DCs and human BDCA3+ DCs are major producers of IFN-lambda in response to poly IC. J Exp Med. 2010; 207:2703–2717. [PubMed: 20975040]
42. Dorner BG, et al. Selective expression of the chemokine receptor XCR1 on cross-presenting dendritic cells determines cooperation with CD8+ T cells. Immunity. 2009; 31:823–833. [PubMed: 19913446]
43. Bachem A, et al. Superior antigen cross-presentation and XCR1 expression define human CD11c +CD141+ cells as homologues of mouse CD8+ dendritic cells. J Exp Med. 2010; 207:1273–1281. [PubMed: 20479115]
44. Schmucker D, et al. Drosophila Dscam is an axon guidance receptor exhibiting extraordinary molecular diversity. Cell. 2000; 101:671–684. [PubMed: 10892653]
45. Watson FL, et al. Extensive diversity of Ig-superfamily proteins in the immune system of insects. Science. 2005; 309:1874–1878. [PubMed: 16109846]
46. Varol C, et al. Intestinal lamina propria dendritic cell subsets have different origin and functions. Immunity. 2009; 31:502–512. [PubMed: 19733097]
47. Bogunovic M, et al. Origin of the lamina propria dendritic cell network. Immunity. 2009; 31:513–525. [PubMed: 19733489]
48. Schulz O, et al. Intestinal CD103+, but not CX3CR1+, antigen sampling cells migrate in lymph and serve classical dendritic cell functions. J Exp Med. 2009; 206:3101–3114. [PubMed: 20008524]
49. Varol C, Zigmond E, Jung S. Securing the immune tightrope: mononuclear phagocytes in the intestinal lamina propria. Nat Rev Immunol. 2010; 10:415–426. [PubMed: 20498668]
50. Manicassamy S, et al. Activation of beta-catenin in dendritic cells regulates immunity versus tolerance in the intestine. Science. 2010; 329:849–853. [PubMed: 20705860]
51. Henri S, et al. The dendritic cell populations of mouse lymph nodes. J Immunol. 2001; 167:741–748. [PubMed: 11441078]
52. Sharpe AH, Wherry EJ, Ahmed R, Freeman GJ. The function of programmed cell death 1 and its ligands in regulating autoimmunity and infection. Nat Immunol. 2007; 8:239–245. [PubMed: 17304234]
53. Travis MA, et al. Loss of integrin alpha(v)beta8 on dendritic cells causes autoimmunity and colitis in mice. Nature. 2007; 449:361–365. [PubMed: 17694047]
54. Posselt G, Schwarz H, Duschl A, Horejs-Hoeck J. Suppressor of cytokine signaling 2 is a feedback inhibitor of TLR-induced activation in human monocyte-derived dendritic cells. J Immunol. 2011; 187:2875–2884. [PubMed: 21844389]
55. Yagil Z, et al. The enigma of the role of protein inhibitor of activated STAT3 (PIAS3) in the immune response. Trends Immunol. 2010; 31:199–204. [PubMed: 20181527]
56. Minas K, Liversidge J. Is the CD200/CD200 receptor interaction more than just a myeloid cell inhibitory signal? Crit Rev Immunol. 2006; 26:213–230. [PubMed: 16928187]
57. Chen M, et al. Dendritic cell apoptosis in the maintenance of immune tolerance. Science. 2006; 311:1160–1164. [PubMed: 16497935]
58. Stranges PB, et al. Elimination of antigen-presenting cells and autoreactive T cells by Fas contributes to prevention of autoimmunity. Immunity. 2007; 26:629–641. [PubMed: 17509906]
59. Kissenpfennig A, et al. Dynamics and function of Langerhans cells in vivo: dermal dendritic cells colonize lymph node areas distinct from slower migrating Langerhans cells. Immunity. 2005; 22:643–654. [PubMed: 15894281]
60. Yamagata T, Mathis D, Benoist C. Self-reactivity in thymic double-positive cells commits cells to a CD8 alpha alpha lineage with characteristics of innate immune cells. Nat Immunol. 2004; 5:597–605. [PubMed: 15133507]

61. Irizarry RA, et al. Summaries of affymetrix GeneChip probe level data. Nucleic Acids Research. 2003; 31
62. Reich M, et al. GenePattern 2.0. Nature Genetics. 2006; 38:500–501. [PubMed: 16642009]
63. Novershtern N, et al. Densely interconnected transcriptional circuits control cell states in human hematopoiesis. Cell. 2011; 144:296–309. [PubMed: 21241896]
64. Reich M, et al. GenePattern 2.0. Nat Genet. 2006; 38:500–501. [PubMed: 16642009]
65. Blatt M, Wiseman S, Domany E. Superparamagnetic Clustering of Data. Physical Review Letters. 1996; 76:3251. [PubMed: 10060920]

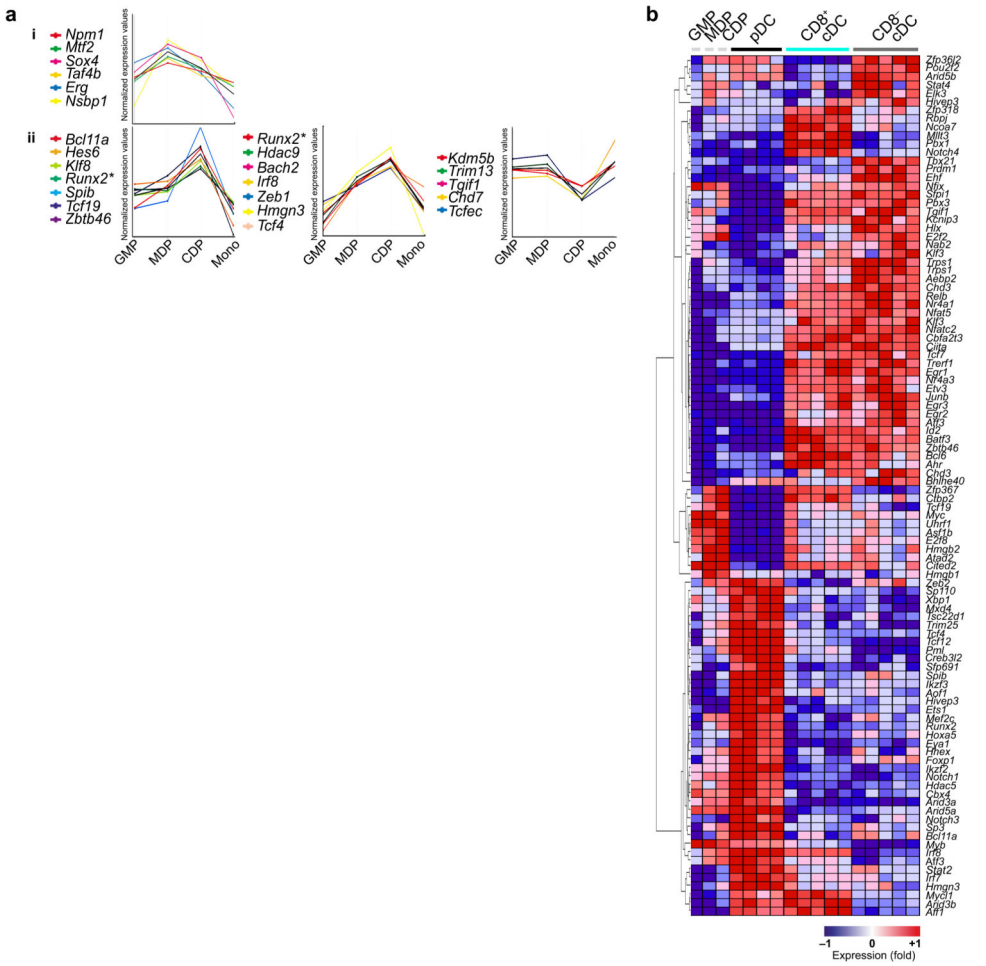

Figure 1.

Transcription factor expression along the DC lineage. (**a**) Graphs show the expression kinetics of transcriptional regulators up-regulated by 1.5 fold at the MDP level (**i**) and up-regulated (FC≥1.5) or down-regulated (FC≤ 0.67) at the CDP level (**ii**) in comparison to its precursor, downstream progeny or nearest neighbor. These regulators were clustered by common patterns of gene expression across the GMP, MDP, CDP, and monocyte families using the Express Cluster program. (**b**) Heatmap representation of Fig. 1a and transcripts up-regulated by at least 1.5 fold at each cellular checkpoint in comparison to their nearest developmental neighbor (cDC versus pDC and $CD8^-$ cDC versus $CD8^+$ cDC) (Fig. S2). Genes are log-transformed, normalized, and centered. Populations and genes were clustered using pairwise centroid linkage with Pearson correlation. Red represents high relative expression, while blue represents low relative expression. *Replicates n ≥3 unless listed otherwise in Table 1.

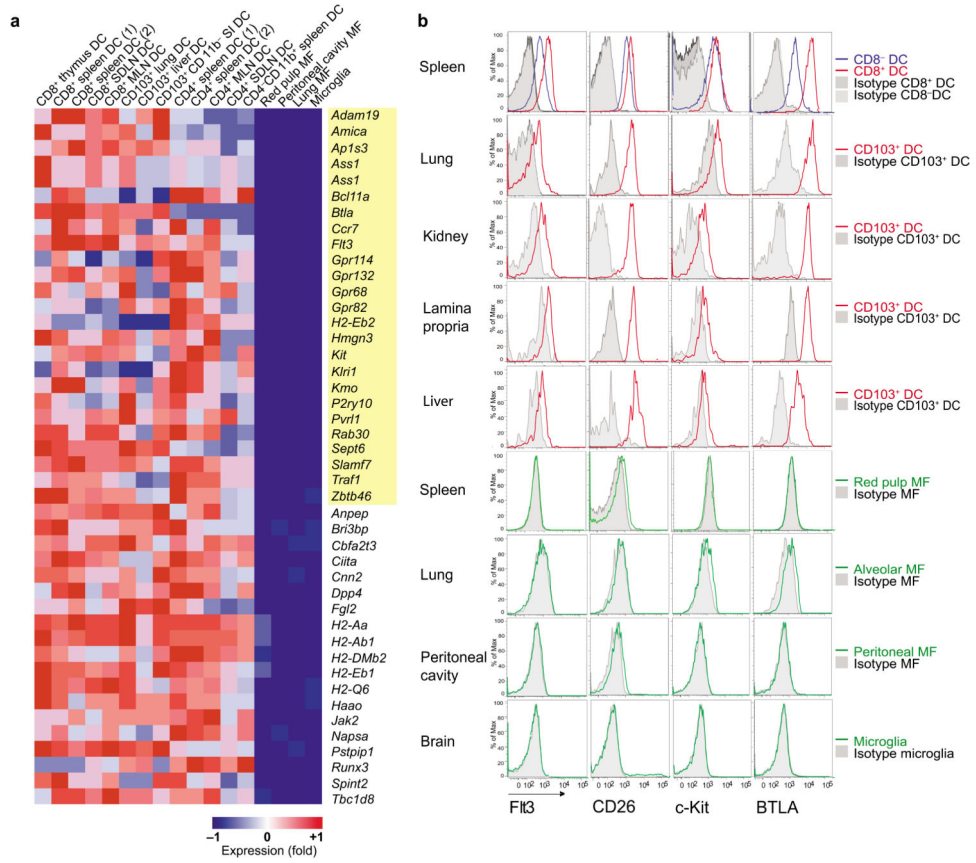

Figure 2.

Identification of gene uniquely expressed or up-regulated in cDC in comparison to MF. (**a**) Heat map exhibits transcripts significantly up-regulated (Student's t-test FDR ≤ 0.05; FC≥ 2) in lymphoid tissue cDC and non-lymphoid tissue CD103$^+$ cDC compared to four prototypical MF populations. Transcripts expressed in cDC and absent in MF according to the QC95 value are highlighted in yellow and form the core cDC signature. Red represents high relative expression, while blue represents low relative expression. Values are listed in Tables 2 and 3. (**b**) Spleen, lung, kidney, lamina propria, liver, peritoneal cavity, and brain single cell suspensions were analyzed by flow cytometry. Histograms show the expression of Flt3, CD26, c0Kit, and BTLA in gated spleen CD8$^+$, spleen CD8$^-$, tissue CD103$^+$ cDC (red/blue lines), and tissue MF (green lines) populations relative to isotype control (gray lines). Data shown are representative of three different experiments. *MLN: mesenteric LN; SDLN: skin draining LN; SI: small intestine.* **Replicates n ≥3 unless listed otherwise in Table 1.

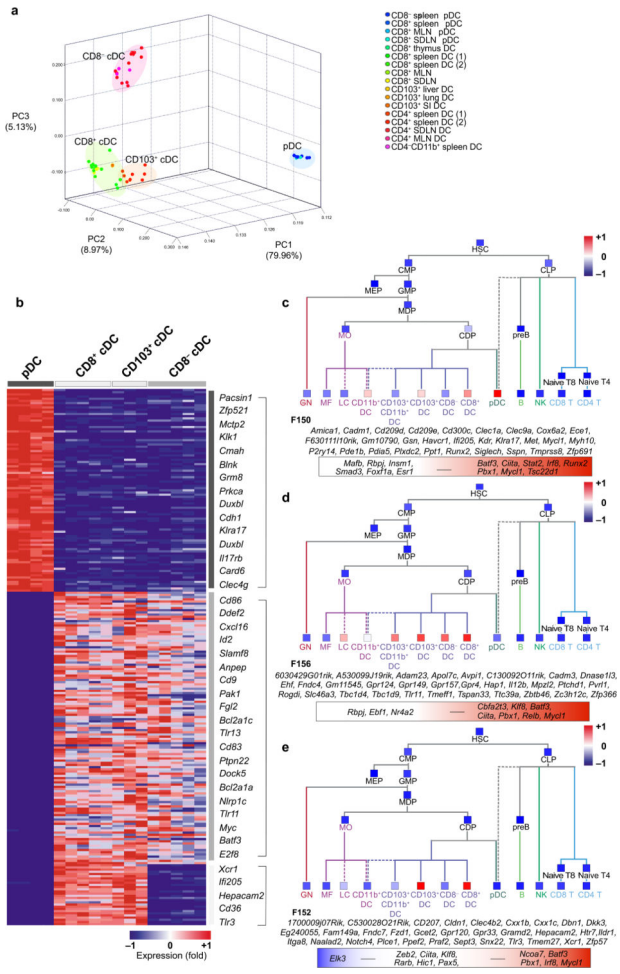

Figure 3.

Unique gene signatures characterize distinct tissue DC clusters. (**a**) PCA of the top 15% most variable genes across pDC, CD8$^+$ cDC, CD8$^-$ cDC and CD103$^+$ cDC transcripts. Replicates are shown. (**b**) Heat map exhibits transcripts significantly (t-test FDR ≤ 0.05) up-regulated by at least two-fold and not expressed in the exclusion population according to the QC95 value in pDC vs cDC, cDC vs pDC, and CD8$^+$/CD103$^+$ cDC vs pDC/CD8$^-$ cDC. Representative genes are listed on the right. Full list is provided in Table S1. Red represents high relative expression, while blue represents low relative expression. (**c**–**e**) ImmGen fine modules consisting of highly co-expressed transcripts and Ontogenet predicted regulators were extracted from the expression dataset representing all hematopoietic cells. Projection of (**c**) Module F150, (**d**) Module F156, and (**e**) Module F152 across the immgen data and mean expression of each module is shown (red colored squares represents high expression, while blue represent low relative expression). The genes expressed in each module are listed in italics below and predicted regulators are displayed in the color box. Red represents predicted activators, while blue represents predicted repressors. *MLN: mesenteric LN; SDLN: skin draining LN; SI: small intestine*. *Replicates n ≥3 unless listed otherwise in Table 1.

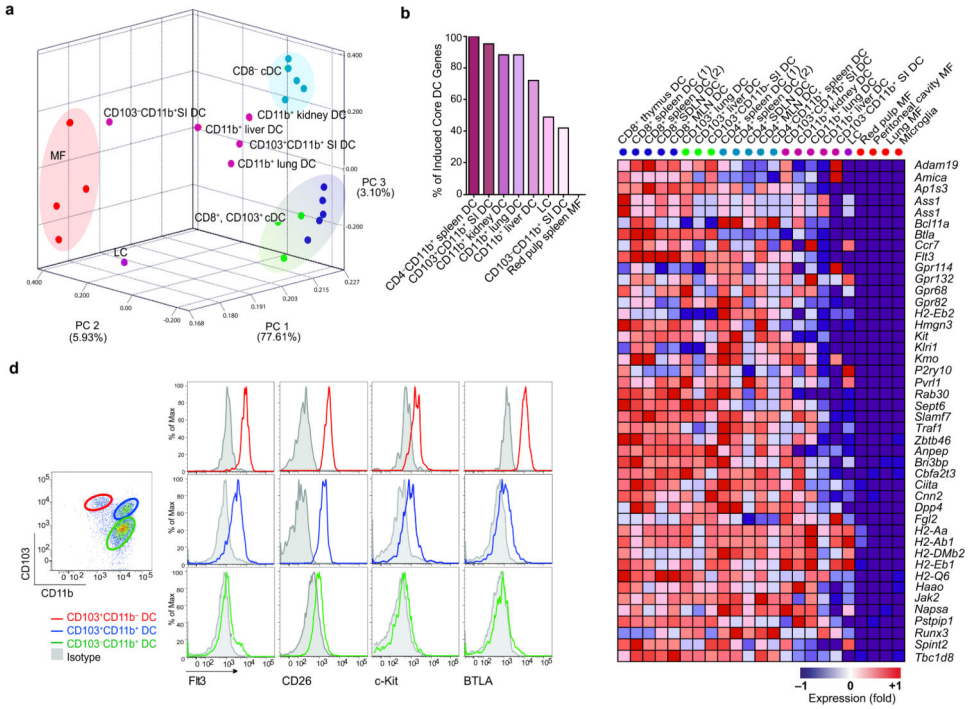

Figure 4.

Non-lymphoid tissue CD11b$^+$ cDC are heterogeneous. (**a**) PCA of the top 15% most variable transcripts expressed by lymphoid tissue CD8$^+$ cDC, CD8$^-$ cDC, non-lymphoid tissue CD103$^+$ cDC, non-lymphoid tissue CD11b$^+$ cDC, epidermal LC and MF. Population means are shown. Population color labels displayed next to heatmap column labels of Fig 4c. (**b**) Graph show percentages of core cDC transcripts (identified in Fig. 2) that are up-regulated (FC≥2) in CD11b$^+$ cDC subsets and red pulp MF. (**c**) Heat map indicates the relative expression of cDC and MF transcripts in each cDC population. Red represents high relative expression, while blue represents low relative expression. (**d**) Small intestine single cell suspensions were analyzed by flow cytometry for core cDC genes. Dot plot shows the expression of CD103 and CD11b on DAPI$^-$CD45$^+$CD11c$^+$MHCII$^+$ lamina propria cDC. Histograms show the expression of Flt3, CD26, c-Kit, and BTLA among CD103$^+$CD11b$^-$ cells, CD103$^+$CD11b$^+$ F4/80$^-$ cells and CD103$^+$CD11b$^+$ F4/80$^+$ cells. Data shown are representative of three different experiments. *MLN: mesenteric LN; SDLN: skin draining LN; SI: small intestine. LC: Langerhans cells.*. *Replicates n ≥3 unless listed otherwise in Table 1.

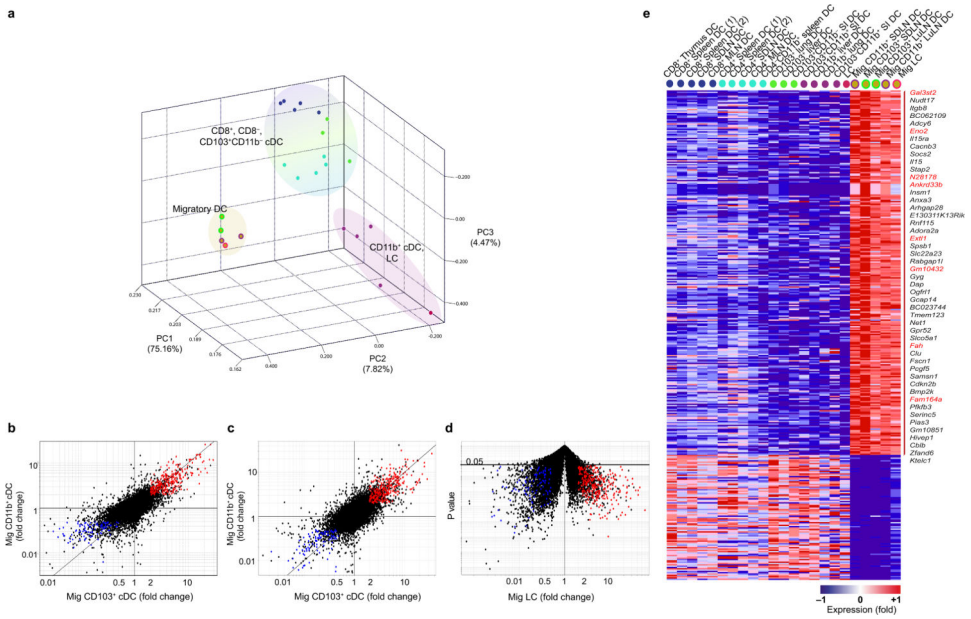

Figure 5.

Tissue migratory cDC up-regulate a unique gene signature regardless of tissue or cellular origin. (**a**) PCA of top 15% most variable transcripts expressed by lymphoid tissue resident $CD8^+$ cDC and $CD8^-$ cDC, non-lymphoid tissue $CD103^+$ cDC, non-lymphoid tissue $CD11b^+$ cDC, epidermal Langerhans cells (LC), migratory (Mig) LC isolated from the skin draining LN, and migratory $CD103^+$ and $CD11b^+$ cDC isolated from skin-draining and lung-draining LN. Population means are shown. Fold change-fold change comparison of gene expression between (**b**) migratory $CD103^+$ cDC and $CD11b^+$ cDC and non-lymphoid tissue resident $CD103^+$ and $CD11b^+$ cDC, (**c**) migratory $CD103^+$ cDC and $CD11b^+$ cDC compared to lymphoid tissue resident $CD8^+$ cDC and $CD8^-$ cDC, and (**d**) migratory LC versus epidermal LC. Red highlights transcripts significantly (FC≥2; t-test p≤ 0.05) increased by at least two–fold, whereas blue highlights those significantly decreased (FC≤ 0.5; t-test p≤ 0.05) in all population comparisons. (**e**) Heat map representation of the transcripts in fold-change fold-change plots from (**b-d**). Genes listed to the right are up-regulated by at least five-fold. Transcripts not expressed in steady state tissue cDC according to the QC95 value in migratory DC vs resident cDC are highlighted in red. Genes in heatmap are listed in Table S2. In heatmap, red represents high while blue represents low relative expression *LuLN: lung draining LN; SDLN: skin draining LN; SI: small intestine, LC: Langerhans Cell*. *Replicates n ≥3 unless listed otherwise in Table 1.

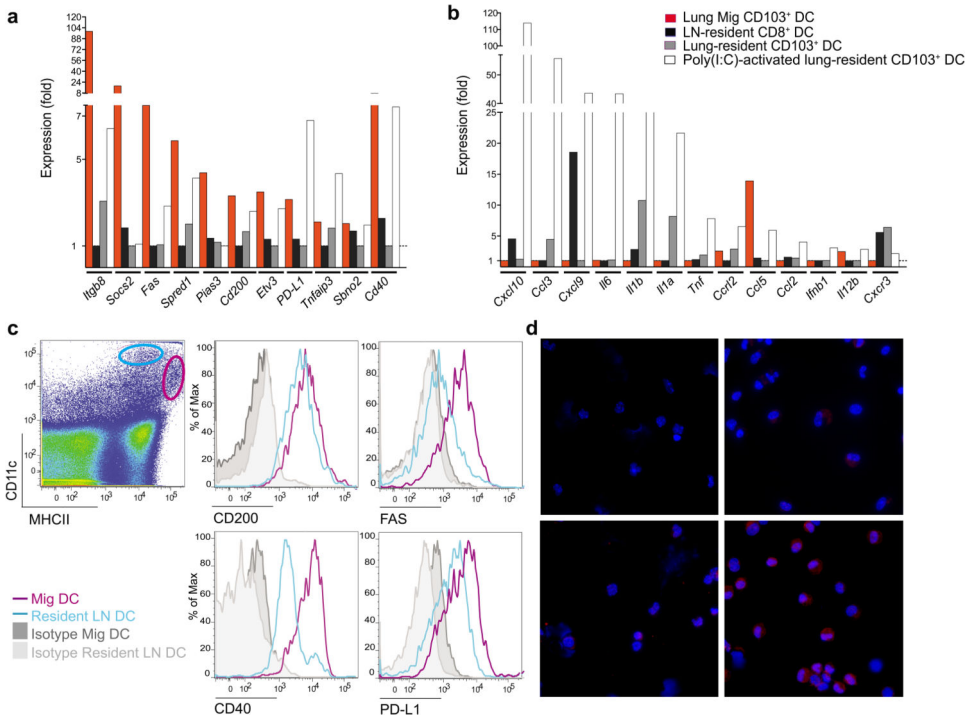

Figure 6.

Tissue migratory cDC express immune dampening genes in the steady state. Bar graphs show fold changes of (**a**) immunomodulatory and Cd40 transcripts, (**b**) inflammatory transcripts in purified lung resident CD103^{+} cDC (gray), Poly: I:C treated lung CD103^{+} cDC (white), LN tissue resident CD8^{+} cDC (black) and lung migratory (Mig) CD103^{+} cDC (red) over the minimum value of the four compared populations. (**c**) LN single cell suspensions were analyzed by flow cytometry. Histograms show the expression of CD200, FAS, CD40, and PD-L1 in gated DAPI^{-}CD45^{+}CD11c^{hi}MHCII^{Int} resident cDC (blue) and DAPI^{-}CD45^{+}CD11c^{int}MHCII^{hi} migratory cDC (pink) compared to isotype controls (gray). (**d**) LN resident cDC (left panels) and migratory cDC (right panels) were sorted, cytospun, and stained with secondary mAb alone (top panels) or anti-Pias-3 mAb (bottom panels). Magnification (63×). *LuLN: lung draining LN; SDLN: skin draining LN; SI: small intestine, LC: Langerhans Cell*. Data shown are representative of three different experiments. *Replicate n ≥3 in graphs unless listed otherwise in Table 1.

Table 1

Cell surface markers used to purify DC and DC precursor populations.

Population	Location	Phenotypical markers																			Replicate Number
		CD45	MHCII	CDllc	CD8	CD4	CDllb	CD103	F4/80	Gr1	B220	Sca1	cKit	Csf1r	Flt3	CD3	CD19	Ter119	Nk1.1	other	
Lymphoid Tissue DC																					
Resident DC																					
CD8+	Skin Draining LN	+		+	+	-	-			-						-	-	-	-	-	3
	Mesenteric LN	+		+	+	-	-			-						-	-	-	-	-	3
	Spleen (1)- NY		+	+	+	-			-		-										3
	Spleen (2)-MA	+		+	+	-	-									-	-	-	-	-	5
	Thymus	+	+	+	+	-	-	+		-						-	-	-	-	-	3
CD8-	Skin Draining LN	+		+	-	+	+			-						-	-	-	-	-	3
	Mesenteric LN	+		+	-	+	+			-						-	-	-	-	-	2
	Spleen (1)- NY		+	+	-	+			-		-										6
	Spleen (2)-MA	+		+	-	+	+			-						-	-	-	-	-	5
	Spleen	+		+	-	-	+			-						-	-	-	-	-	3
Migratory DC																					
Mig CD103+	Skin Draining LN		hi	int	-	-	-	+												Langerin+	3
	Mediastinal LN		hi	int	-	-	-	+													3
Mig CD11b+	Skin Draining LN		hi	int	-	-	+	-												Langerin-	3
	Mediastinal LN		hi	int	-	-	+	-													3
Mig LC	Skin Draining LN		hi	int	-	-	+	-												Langerin+	3
pDC*																					
	Spleen	+		+	+					+	+					-	-		-		3
	Mesenteric LN	+		+	+					+	+					-	-		-		2
	Skin Draining LN	+		+	+					+	+					-	-		-		3
	Spleen	+		+	-					+	+					-	-		-		3
Non-Lymphoid Tissue DC																					
CD103+	Lung	+	+	+			-	+													5
	Liver	+	+	+	-	-	-	+											-		2
	Small Intestine	+	+	+	-	-	-	+	-												4
CD11b+	Lung	+	+	+			+	-													2
	Liver	+	+	+	-	-	+	-											-		3

Population	Location	Phenotypical markers																	Replicate Number
		CD45	MHCII	CDllc	CD8	CD4	CDllb	CD103	F4/80	Gr1	B220	Sca1	cKit	Csf1r	Flt3	CD3	CD19	Ter119	Nk1.1	other	
	Small Intestine	+	+	+	-	-	+	-	+												7
	Kidney	+	+	+			+	-	low	-										NKp46.1-	3
CD103+CD11b+	Small Intestine	+	+	+	-	-	+	+	-	-											4
LC	Skin	+	+	+	-	-	+	-											-	Langerin+	2
Precursors																					
GMP	Bone Marrow						-			-	-	-	hi			-		-	-	CD34+ CD16/32 hi	3
MDP	Bone Marrow						-			-	-	-	hi	+	+	-		-			3
CDP	Bone Marrow						-			-	-	-	lo	+	+	-		-			3
Monocyte	Blood		-							+	-			+						CD43-	3

DC precursors were isolated from the bone marrow, whereas differentiated DC were purified from tissues. DC precursors and tissues DC were purified using FACS based on the expression of the cell surface markers listed here and according to the Immgen standard of operation procedures detailed in the method section.

*Spleen pDC include a $CD8^{+}$ and $CD8^{-}$ subset

Table 2
List of transcripts up-regulated in cDC and absent from MF

cDC vs MF	cDC Ave	MF Average
Adam19	1119+/-259.2	94.3+/-6.1
Amica1	702.6+/-216.9	45.5+/-3.1
Ap1s3	642.4+/-111.2	43.7+/-7.1
Ass1	905+/-234.2	69.8+/-2
Bcl11a	940.1+/-262.9	95.3+/-9.3
Btla	1481.7+/-413.3	49.4+/-3.9
Ccr7	1012+/-251.5	81.3+/-7.2
Flt3	3408.4+/-370.3	66.3+/-11
Gpr114	406.6+/-132.9	57.1+/-3.9
Gpr132	1007.6+/-127.9	84.1+/-5.2
Gpr68	289.4+/-61.4	52.5+/-4.8
Gpr82	67.7+/-18.2	11.7+/-0.8
H2-Eb2	782.2+/-371.1	43.4+/-5.5
Hmgn3	153.6+/-25.3	23.1+/-2.5
Kit	2368.3+/-375.7	67.7+/-6.1
Klri1	527.4+/-204.7	17.2+/-0.5
Kmo	1160.4+/-212.6	20.7+/-1.1
P2ry10	519.2+/-152.7	19.6+/-2.2
Pvrl1	475.6+/-54.3	74.4+/-6.1
Rab30	289.2+/-52.8	28.7+/-3.6
Sept6	1080.3+/-202.3	99.2+/-12.4
Slamf7	1727.4+/-145.6	31.7+/-5.2
Traf1	1044.4+/-224.5	51.6+/-2.8
Zbtb46	400.8+/-54.2	93.8+/-10.3

The transcriptome of cDC excluding non-lymphoid tissue $CD11b^{+}$ cDC subsets was compared to four MF populations (red pulp MF, alveolar MF, peritoneal cavity MF and microglia) to identify transcripts that were significantly (t-test FDR ≤ 0.05) up-regulated by at least two fold and not expressed in MF according to the QC95 value. Transcript expression average +/- the standard error of the mean in cDC and MF are listed

Table 3
List of gene transcripts up-regulated in cDC

cDC vs MF	DC Ave	MF Average
Anpep (Cd13)	1682.8+/-197.7	87.1+/-20.7
Bri3bp	814.3+/-86.3	177+/-44.1
Cbfa2t3	1266.3+/-100.8	208.5+/-52.5
Ciita	1692+/-190.1	121.4+/-46.8
Cnn2	1884.8+/-271.2	230.7+/-54.7
Dpp4 (Cd26)	2567.1+/-360	72.3+/-29.6
Fgl2	1276.4+/-326	90.2+/-26.3
H2-Aa	13267.3+/-555.7	1632.6+/-1173.7
H2-Ab1	10299.7+/-490.6	1093.6+/-755.3
H2-DMb2	2491.8+/-305.6	400.5+/-67.6
H2-Eb1	7165.4+/-608	704.4+/-458.9
H2-Q6	1481.4+/-149.9	288+/-48.4
Haao	653.2+/-59.4	152.3+/-24.9
Jak2	2300+/-234.7	331.9+/-51.5
Napsa	1616.4+/-237	190.9+/-49.7
Pstpip1	475.1+/-42.7	104.4+/-16.4
Runx3	672.8+/-151.1	100.9+/-11.3
Spint2	773.6+/-166	139.4+/-8.4
Tbc1d8	2009.8+/-209.5	219.3+/-75.8

The transcriptome of cDC excluding non-lymphoid tissue CD11b^{+} cDC subsets was compared to four MF populations (red pulp MF, alveolar MF, peritoneal cavity MF, and microglia) to identify transcripts that were significantly (t-test FDR ≤ 0.05) up-regulated by cDC compared to MF. Transcript expression average +/- the standard error of the mean in cDC and MF are listed.